RESEARCH ARTICLE

Properties and perspective applications of copper sulfide nano-materials: a review

Ofeliya Balayeva

Dr

Baku State University

Azerbaijan

Email: educ25000@gmail.com

Doi Serial https://doi.org/10.56334/sei/8.6.66

Keywords Copper sulfide, nanostructures, optical properties, structural properties, energy stor- age and conversion (ESC) devices.

Abstract

In this review we could get more information about nanostructured copper sulfide, its properties and applications in many fields. The key reaction parameters that influence the nucleation and growth as well as the size, shape, composition, and structure are carefully discussed.

Citation

Balayeva O. (2025). Properties and perspective applications of copper sulfide nano-materials: a review. *Science, Education and Innovations in the Context of Modern Problems*, 8(6), 603-614; doi:10.56352/sei/8.6.66. https://imcra-az.org/archive/364-science-education-and-innovations-in-the-context-of-modern-problems-issue-6-volviii-2025.html

PACS: 61.46.

Science, Education and Innovations in the Context of Modern Problems, Issue 6, Vol.VIII, 2025

Received: 05.02.2025	Accepted: 29.04.2025	Published: 28.05.2025 (available online)

Introduction

Semiconductor nanocrystals are always metastable phases, and they should be passivated byligands to avoid aggregation, though it is hard to meet this goal by the above mentioned solid-solid or solid-gas reactions. Nanocrystalline copper sulfide exhibits at least five stable phases with different Cu:S molar ratios. These phases include covellite (CuS), anilite ($Cu_{1.75}S$), digenite ($Cu_{1.8}S$), djurlite ($Cu_{1.95}S$), and chalcocite (Cu_2S) [1]. Copper sulfide grows with 0-D (quantum dots [2,3], 1-D (nanotubes [4,5]; nanowires [6-8]; nanorods [9,10]; nanoneedles [11,12]), 2-D (nanoplates [13-15]; nanoribbons [16,17];

nanodisks [17]; nanosheets [11,18]) and 3-D (nanocubes [19], nanospheres [20-23], cages [24, 25]. Therefore, there is a strong tendency to minimize the total surface energy. Owing to its unique electronic, optical and other physical and chemical properties [26, 27] and wide potential applications in many fields[28], copper monosulfide (CuS) semiconductor has attracted much attention.

Among these various morphologies, hollow spheres with nano- or microsized dimensions gain ex- tensive attentions because of its prospective applications in catalysis, drug delivery, light fillers, chemical storage and photonic crystals [29-31].

In this review we could get more information about nanostructured copper sulfide, its propertiesand applications in many fields. The key reaction parameters that influence the nucleation and growth as well as the size, shape, composition, and structure are carefully discussed.

1. Properties of Copper Sulfide Nanomaterials. Owing to its unique elec- tronic, optical and other physical and chemical properties [26, 27] and wide potential applications in many fields [28], copper monosulfide (CuS) semiconductor has attracted much attention. In this section, we will selectively summarize the main and general properties

of copper sulfide nanomaterials.

1.1. Structural properties. The crystal structure of covellite is hexagonal (space group P63/mmc, a

= 380 pm, c = 1640 pm) with 6 CuS formula units in the unit cell. Of the 6 Cu atoms 4 are tetrahedrally coordinated and 2 are triangularly coordinationed by S atoms. Four of the 6 S atoms form S groups. In accordance with this, the S (2p) X-ray photoelectron spectrum of CuS shows a doublet structure corre- sponding to the two different coordinations (octahedrally and triangularly bipyramidal) of S atoms [32- 34]. The electron-diffraction results presented can, however, be readily interpreted as a mixture of hex- agonal chalcocite and high digenite [35]. Kimihiko Okamoto et al. [36] observed what they denoted as "indistinct polymorphic phase transitions" in the temperature region 90 to 310 K. Such transitions have not been confirmed by other investigators. The heat capacity was extrapolated to the decomposition tem- perature of covellite, 780 K [34].

Both the precursor molar concentration, reaction time and the reaction temperature are crucial for obtaining pure CuS. CuS and Cu_2S hydrothermally synthesized at (a) 150 °C, (b) 180 °C, and (c) 250 °C with varied precursor [$Cu(NO_3)_2$: $Na_2S_2O_3$] molar ratios [13]. The XRD patterns of the product obtained with a [$Cu(NO_3)_2$: $Na_2S_2O_3$] = 1 : 2 molar ratio at 150 and 180 °C are found to be similar and well- matched to pure hexagonal CuS. However, the product obtained at 250 °C shows two additional diffrac- tion peaks, which are assigned to Cu2S along with the major hexagonal CuS diffraction peaks. The rela- tively high pressure generated during the high temperature (250 °C) hydrothermal synthesis leads to the desulfurization of some CuS to Cu2S. Further increasing the thiosulfate concentration, i.e., 1 : 6 molar ratio of $Cu(NO_3)_2$ to $Na_2S_2O_3$, they obtained CuS along with sulfur at all three reaction temperatures.

This is obviously due to the excess amount of thiosulfate in the reaction medium [13]. An optimum pre- cursor [$Cu(NO_3)_2$: $Na_2S_2O_3$] molar ratio of 1 : 2 is suitable for synthesizing pure CuS in the temperature range of 150–180 °C, whereas with a molar ratio of 1 : 4, the synthesis temperature should be higher than 200 °C, so the excess sulfur formed could be degraded. However, Changhua An et al. reported pure CuS with a 1 : 6 precursor molar ratio of copper acetate and sodium thiosulfate in ethylene glycol solvent and sodium oleate and hexadecylamine as surfactant at 180 °C [37]. This suggests that, in aqueous medium, is suitable for obtaining pure CuS in a shorter reaction time with a lower thiosulfate precursor concentra- tion.

1.2. Optical properties. In the Cu–S system, it has many known stable phases from chalcocite (Cu_2S) to sulfur-rich covellite (CuS). Each stable phase has its own characteristic optical property. UV– visible absorption spectroscopy is a useful technique to monitor the optical properties of the nanomateri- als. Semiconductor nano-crystallites are known to have an absorption edge, which is shifted with respect to the bulk material towards shorter wavelengths. This blue shift is thus taken as an indication of the presence of such nanocrystals, and can be used to evaluate the crystallite size [38]. In a previous study, CuS nanowires [6] have been reported by hydrothermal method. Optical absorption of it is reported; the product obtained at lower temperature (120–175 °C) with CuS nanowire shows a small absorption peak around 400 nm and has broad absorption in the near-IR.

For some Cu–S system nanoparticles [39] they point out to have two phases (CuS and Cu_2S), the presence of a characteristic broad absorption band in UV region for Cu_2S and the other in near-IR region for covellite copper sulfide (CuS).

Such a copper sulfide group (Cu_xS) involves various compounds, Cu_2S (chalcocite), $Cu_{1.96}S$ (djur- leite), $Cu_{1.8}S$ (digenite) and CuS (covellite). The electronic structures depend on their stoichiometries,i.e., the copper deficiency. $Cu_{1.96}S$, $Cu_{1.8}S$ and CuS are of a direct band gap type, while Cu_2S is of an in- direct band gap type. The energy band gap varies from 1.2 eV for x = 2 and 1.5 eV for x = 1.8 to 2 eV forx = 1 [40]. Since their optical properties also depend on the size and shape of copper sulfide nanocrystals,it is important to control their morphology and composition for application to optoelectrical devices.

For the CuS nanoparticles prepared at (a) 150 °C, (b) 180 °C, and (c) 250 °C with a precursor molar ratio of 1 : 2 [$Cu(NO_3)_2$: $Na_2S_2O_3$] [13] a broad peak is observed in the region of 600–650 nm for the CuSprepared at 150 and 180 °C, whereas the CuS prepared at 250 °C shows a peak at ~675 nm. The measured bandgap is 1.75 eV for CuS prepared at 150 °C whereas it is 1.68 eV for CuS prepared at 180 and 250 °C suggesting potential applications in optoelectronic devices.

The hot injection method used 1-octadecene and tri-n-octylphosphine solution medium, cuprous acetate and dodecanethiol precursors to synthesize Cu_2S nanodisks at 160–220 °C, and the size and as- pect ratio could be controlled by changing refluxing temperature and time [23]. The band gap of the products plotted as a function of reaction temperature shows a gradual decrease from 1.53 to 1.36 eVwith increasing temperature. The decrease of the band gap is ascribed to the increased size of Cu_2S nanocrystals at higher reaction temperatures (Fig. 1).

The growth of Cu_2S nanocrystals has been monitored by characterizing samples collected at differ- ent reaction times by using TEM and UV-vis absorption spectroscopy. The diameter/thickness of Cu_2S disks changed from 13/7.5 nm to

18.2/9.6 nm gradually when the reaction time extended from 60 to 300 min [23]. After the relatively fast nucleation at around 15 min, the slow growth of Cu_2S nanocrystals gradually strengthened the absorption of the nanocrystals, leading to a red shift of the peak as the reaction proceeds. The relatively fast nucleation and slow growth processes are believed to contribute to the high uniformity of the nanocrystals [41]. One can notice slight broadening in size for samples heated for along time (e.g., 540 min) because of the Ostwald ripening process. The final product after 540 min of reaction shows a very broad absorption spanning from UV to near IR which may make this material a good candidate for photovoltaic devices.

1.3. Thermal properties. The presence and degradation of elemental sulfur formed with CuS was characterized by thermal analysis [$Cu(NO_3)_2$ and $Na_2S_2O_3$] molar ratios [13]. They were heated CuS at different temperatures in a vacuum

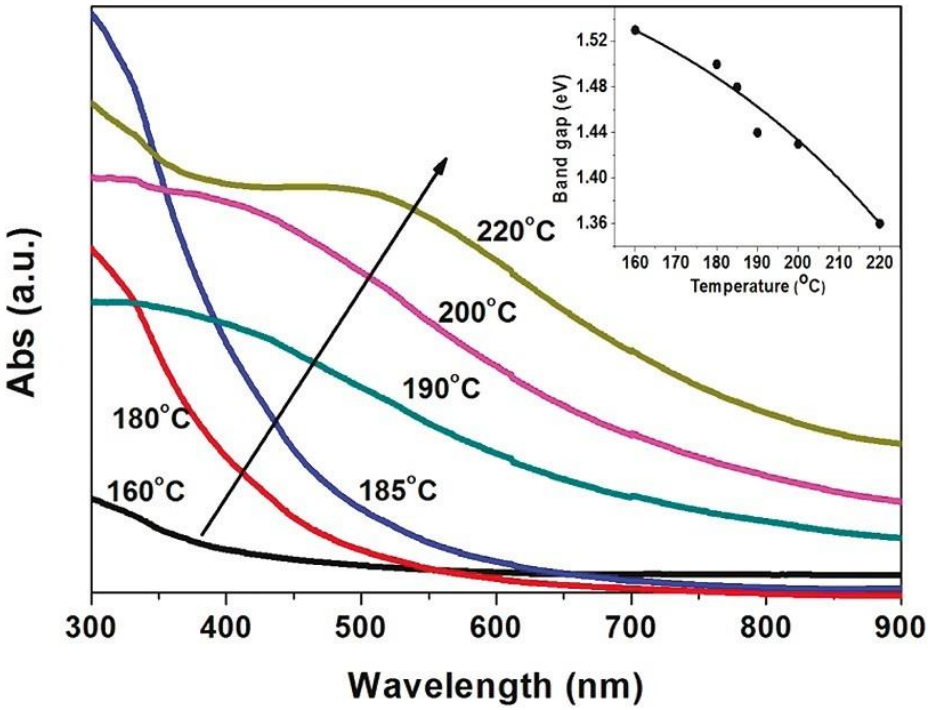

and/or in air and found different results (figure 2). The residue ob- tained upon calcining pure CuS at 350 °C shows the formation of Cu_2S, which is in accordance with the TG analysis. However, the pure CuS product calcined at 400 and 450 °C produced copper sulfate hydrox-ide hydrate and copper sulfate hydroxide, as shown in Fig.2. According to fig 2. the oxygen present for formation of CuO at 800 °C. Upon heating the pristine CuS to 350°C in a vacuum, a Cu_2S phase emerges[13].

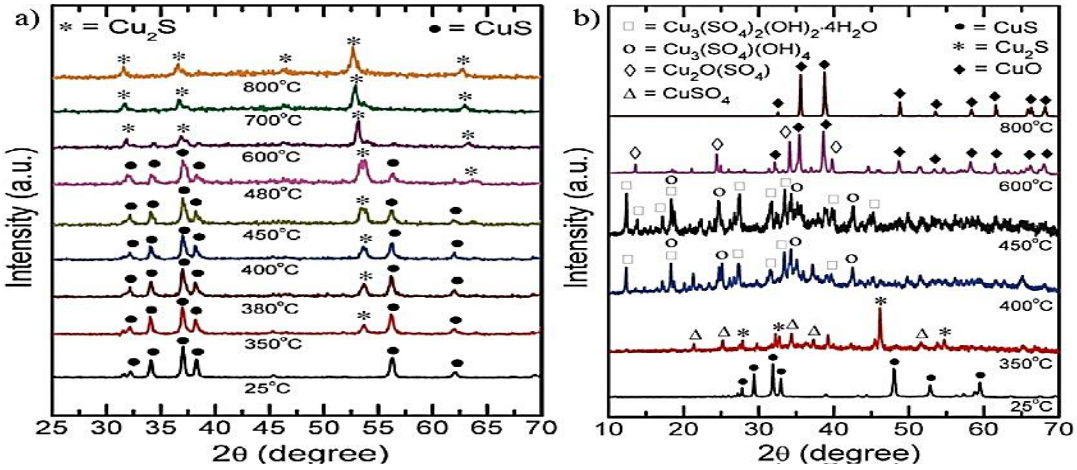

Figure 1. *UV-Vis-NIR absorption spectra of Cu2S nanocrystals obtained at different reaction tem-peratures; the inset shows variation of band gap as a function of reaction temperature.* [23]

Fig. 2. *(a)XRD patterns of CuS heated at different temperatures in a vacuum. High temperatureheating induced the phase*

change of CuS to Cu_xS. (b)XRD patterns from the residues of pure CuS cal-cined at different temperatures in air.

This is in accordance with the thermal analysis, which shows the desulfurization of CuS to Cu_2S. Upon further increasing the temperature up to 480 °C, the intensity from Cu_2S diffraction features is found to increase, which indicates more desulfurization of CuS to Cu_2S. It is also important to note that the most intense diffraction feature of Cu_2S, at 2θ of ~54°, is found to be shifted to a lower 2θ with an increase in the temperature of the sample. This is due to the lattice expansion of the crystal at higher tem-peratures [13].

Liqiu Wang et al. [42] apply the chemical solution method to synthesize CuS/Cu_2S nanofluids andexperimentally measure their thermal conductivity. The measured thermal conductivity shows that the presence of nanoparticles can either upgrade or downgrade fluid conductivity, a phenomenon predicted by the recent thermalwave theory of nanofluids. The presence of CuS/Cu_2S nanoparticles can either en- hance or weaken fluid heat conduction so that the conductivity ratio varies from 0.82 (smaller than 1) to

1.21 (larger than 1).

1.4. Electrical properties/ Photoelectric and Thermoelectric properties. Electrochemical capaci-tors (ECs), also called supercapacitors, are attracting particular attention owing to their high power den- sity, rapid charging/discharging rate, and long cycle life. ECs are divided into two types, depending on their underlying energy storage mechanism- electrical double-layer capacitors (EDLCs) and pseudo ca- pacitors [43]. Whereas EDLCs store electrical energy by the electrostatic accumulation of charges in an electric double-layer close electrode/electrolyte interfaces, pseudo capacitors exploit reversible Faradaic reactions that occur at the electrode surface, and so have a much higher specific capacitance [44]. Coppersulfide is one of the promising cathode materials of lithium ion batteries (LIBs) because of its advantagesof a high theoretical capacity 560 mAh g^{-1}, flat discharge curves and a good electrical conductivity (10^{-3} S cm^{-1}) [45]. As an important semiconductor material, copper sulfides exhibit their unique physical and chemical properties. For instance, copper sulfide (covellite) shows a metal-like electrical conductivity

[46] and transforms into a superconductor at 1.6 K [47]. Anup Mondal et al [48] reported a chemical route for the deposition of nanocrystalline thin films of CuS, using aqueous solutions of $Cu(CH_3COO)_2$, $SC(NH_2)_2$ and $N(CH_2CH_2OH)_3$ [triethanolamine, i.e. TEA] in proper concentrations and ratios. For elec- trical characterizations, the CuS films were deposited on fluorine doped tinoxide (SnO_2:F) coated trans- parent conducting oxide (TCO) glass substrates and the d.c. I–V measurements within the range of -3.0 Vto +3.0 V were carried out. The upper electrical contact to the film was made with carbon paste of 0.09 cm^2 area, while, TCO itself acted as the bottom contact [48].

A. P. Alivisatos et al. fabricated a hetero-junction of Cu_2S on indium-tin-oxide glass and flexible plastic substrates by spin coating to study it's photovoltaic performance [49]. Jeunghee Park et al. re- ported polymer solar cells using Cu_2S-MWCNTs nanocrystals [50]. For the photovoltaic application, it is important to fabricate the materials as thin film forms. Copper sulfide thin films can be obtained directly by electrochemical or atomic layer deposition processes [51] or drop-casted to fabricate a thin film. Glass, polyester, and metals are generally used as the substrate for depositing thin films of Cu_xS [52].

1.5. Field-emission (FE) properties. As compared with conventional technologies, nanostructures have many advantages such as faster device turn-on time, sustainability and compactness [53]. Recent progress in the research on FE and stimulated emission properties of 1D wide band-gap semiconducting metal sulfide nanostructures has resulted in an important increase in the current density and decrease in the turn-on voltage [54]. Hierarchical microrings and porous microrings were synthesized through a fac- ile solvothermal method by Ke Yu et al. [55]. In some recent researches, FE properties of Cu_2S nanos- tructures with different morphologies were reported [56].

Ke Yu et al. investigated the FE properties of self-mosaiced Cu_2S nanoflowers and compared them to those of the original self-assembled nanoflower sample [57]. For FE measurement, self-mosaic and original self-assembled Cu_2S samples were painted on Si substrates by a screen-printing method respec- tively. FE properties were measured under a high vacuum level of about 2×10^{-5} Pa at room temperature. The emission area was 1cm×1cm. Generally, FE mainly depends on the emitter geometry [58]. The Cu_2S nanostructures with thin edges on the surface are supposed to have good FE properties. The emission cur-rent density exponentially increases with the increase of applied field. The turn-on field and threshold field for original and self- mosaic Cu_2S samples are about 5.2V/μm and 8.4V/μm, 4.4V/μm and 7.6V/μm, respectively. It is clear that the FE property for the self-mosaic Cu_2S sample is better than the other one. In the case of their self-mosaic Cu_2S sample, the applied primary field gets enhanced on the original nanosheets, which successively act as a secondary field for the small self-mosaiced nanosheets, thereby enhancing the local electric field. For these reasons, self-mosaic Cu_2S sample shows better FE properties. Three flower-like and one rod-shape cubic Cu_2S nanostructures were successfully synthesized from a facile hydrothermal method [59]. Field emission (FE) properties of these nanostructures results indicated that the tetragonal $Cu_{1.81}S$ nanorods had excellent field emission performance with turn-on field of ~2.2V μm^{-1}, threshold field of ~5.1 V μm^{-1} and enhancement factor of 1532. It showed that the tetragonal $Cu_{1.81}S$ nanostructures were competitive material in FE applications. The $Cu_{1.81}S$ nanoparticles have lower work function than Cu_2S. Therefore, it is

reasonable that electrons can be emitted more easily from these sharp edges of $Cu_{1.81}S$. Moreover, the result shows that nanorods own better emitter geometry than nanoflowers and the field emission property for the $Cu_{1.81}S$ nanorods compares favorably with that of the multiwall CNTs [60].

1.6. Photocatalytic activity. Nanostructured semiconductors have faster electron migration and charge generation rate due to their higher surface area-to-volume ratio than the bulk [61]. Semiconductor nanomaterials for photocatalytic degradation of organic contaminants are promising materials in envi- ronmental protection nanotechnology [54]. The development of new visible light-active photocatalysts is one of the most important subjects in photocatalysis research. Doping of metal ions into wide band gap metal sulfide semiconductor nanomaterials has been used to prepare photocatalysts [62].

The photocatalytic performance of the hierarchical CuS structures on the oxidation of methylene blue (MB) dye has been studied in the presence of hydrogen peroxide [63]. The catalytic reaction was conducted under natural light. UV–Vis spectra were applied to demonstrate the photocatalytic degrada- tion activity of MB. The intensity absorption peak at 662 nm of MB decreased gradually with the exten- sion of time, indicating the photocatalytic degradation of MB. About 90% of the MB was degraded after 90 min (**fig. 3**). In their work, the hierarchical CuS structures have a lot of unfolded nanoplates that could absorb more photons to produce electron–hole pairs under natural light, and the deep and capacious pores enable the hierarchical structures to be exposed to the MB solution sufficiently. Furthermore, the nano-size of plates could reduce the radiationless recombination of electron–hole pairs [64], which is also in favour of the photocatalysis of MB.

Currently, the studies on the photocatalytic properties of CuS nanostructures are seldom reported. G.C.Guo et al. [65] reported the photocatalytic properties of CuS nanoflowers on Rhodamine B and the degradation rate is close to 90% after 2 h halogen lamp irradiation.

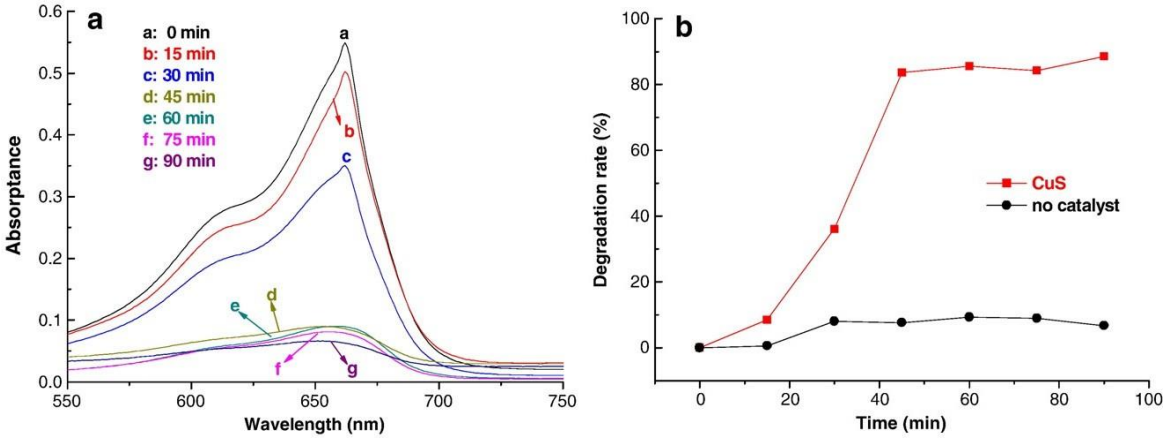

Fig. 3. *(a) Absorption spectra of MB aqueous solutions in the presence of the hierarchical CuSstructures. (b) Degradation rate of MB at different intervals [63].*

Andrews Nirmala Grace et al. explained the mechanism of photocatalytic reaction in their work [66]. They prepared CuS nanostructures by hydrothermal route using copper nitrate and thiourea as cop- per and sulfur precursors. The photocatalytic activity was evaluated by the decolorization of methylene blue (MB) dye under visible-light irradiation and results showed that 87% of the dye was degraded. The photocatalytic degradation of methylene blue was monitored under visible light irradiation and the meas- urement was taken using a UV–Vis spectrophotometer [66]. For the adsorption of dye molecules, elec- tron–hole pair plays an important factor. Initially the dye molecule gets adsorbed on the surface of the catalyst. When CuS photocatalyst absorbs light from the visible region, it will produce pairs of electrons and holes, which further react with dye molecules to oxidize the dye pollutant into non-toxic products. Under visible light radiation, an electron from the valence band gets excited to conduction band to form electron–hole pairs. The electrons from the conduction band are transferred to the catalyst surface reducing O^{2} to O^{2-} [66]. On the other hand, the holes in the valence band react with H_2O on the surface of the catalyst to form hydroxyl radicals. These radicals show high oxidizing ability reacting with organic dyes to oxidize it. Thus the as-prepared CuS catalysts are highly promising materials for photocatalytic appli- cations towards dye degradation.

High quality CuS and CuS/ZnS core/shell nanocrystals (NCs) were synthesized in a large quantity using a facile hydrothermal method at low temperatures of 60 °C and evaluated in the photodegradationof Rhodamine B (RhB) under visible light irradiation [67]. Photocatalytic activity originates from photo- generated holes in the narrow bandgap CuS, with encapsulation by large bandgap ZnS layers used to form the core/shell structure that improves the resistance of CuS towards photocorrosion. Such CuS/ZnS core/shell structures exhibit much higher photocatalytic activity than CuS or

ZnS NCs alone under visi- ble light illumination, and is attributed to higher charge separation rates for the photo-generated carriers in the core/shell structure [67]. The high photodegradation efficiency of CuS/ZnS core/shell catalysts can be explained by the formation of type-II structure, which promotes the separation of the photoexcited electrons and holes which contribute to the photocatalytic decomposition reaction of RhB. The stability of the CuS/ZnS core/shell particles and impact of the ZnS shell in resisting photocorrosion was verified by exploring the reusability of the photocatalyst. After five photodegradation recycles of RhB, the CuS/ZnS core/shell catalysts did not display any significant loss in the photocatalytic activity, confirming that CuS/ZnS core/shell NCs were good photocatalytic materials. These materials open up exciting op- portunities for visible light initiated photocatalytic depollution and subsequent studies will evaluate the application of these catalysts under continuous operation [67].

2. Perspective applications. Nanostructured copper sulfide exhibit size and shape de- pendent properties and have potential applications in various fields, such as materials science; biomedical science [4,68]; electronics[69,70]; optics [71]; energy storage [20], electrochemistry [69,70] and so on.As a typical transitional metal chalcogenide, copper sulfide is a well known p-type semiconductor thathas potential in applications of solar controller, solar radiation absorber and lithium ion batteries [72,73].

Synthetic colors are widely used in food industries; while some of them may generate [74] hazards and problem to human health at excess level [74]. Reza Sahraei et al. [75] were synthesized copper sul- fide nanoparticles loaded on activated carbon (CuS-NP-AC) by novel, low cost and green approach was used for the removal of sunset yellow (SY) from aqueous solutions. Another resembling work, Mehro- rang Ghaedi et al. synthesized CuS-NP-AC adsorbent was utilized to removal of AO (Auramine O (4,4'- dimethylaminobenzophenonimide) and SO (Safranin O -2,8-dimethyl-3,7-diaminophenazine) dye from aqueous medium in presence of ultrasound radiation [76]. It was found that application of ultrasound leads to significant enhancement in extent of adsorption and removal percentage of AO and SO from aqueous solutions. Combination of ultrasound with CuS-NP-AC increased the dye removal percentage (more that 99%) by using small amount of adsorbent (0.06 g) in short time (7 min). The proposed method has good potential for removal of dyes from waste water compared to several other adsorbents.

Special rose-like copper (I) sulfide nanostructure (Cu_2S NRS) made up of thickness nanoplates were successfully synthesized on copper rod by a simple method can be used as integrated electrode (called as Cu_2S NRS/CRIE) to nonenzymatic detect the cholesterol (CT) [16] In the past, many works were devote to fabricate enzyme-based sensors because it's high sensitivity and good selectivity [77,78], but the activity of the enzyme decreases with use and the enzymeis easily denatured during its immobili- zation procedure due to its intrinsic instability and the activity of the enzyme is liable to be affected by pH, temperature and toxic chemicals. Moreover, the reproducibility of enzyme-based sensors is not very good and needs to be further improved [79]. In the [16] work results show the Cu_2S NRS/CRIE displayed excellent performance, a wide linear range from 0.01 mM to 6.8 mM for the detection of cholesterol with a low detection limit of 0.1 μM(S/N = 3).

Glucose detection is extremely important for diabetes clinical detection and therapy [80]. In recent years, variety of Cu based nanomaterials have been reported toward the development of nonenzymatic glucose sensors [81], but the nonenzymatic glucose sensor based on hollow structured CuS was rarely reported. There are several methods reported for the synthesis of the CuS nanotubes such as oleic acid/water microemulsion method and microwave assisted Cu complex transformation method [82]. In these two reports, the as-prepared CuS NTs could be used for nonenzymatic glucose sensing at low glu- cose concentration with high sensitivity [4].

2.1. Application in energy storage and conversion (ESC) devices.

2.1.1. Batteries. Copper sulfides have been investigated as battery active materials for lithium-ion batteries (LIBs) for several decades. Cu_2S nanocrystals are widely used in LIBs. Owing to the increasing demand of energy and shifting to the renewable energy resources, (LIBs) have been considered as the most promising alternative and green technology for energy storage applied in hybrid electric vehicles (HEVs), plug-in hybrid electric vehicles (PHEVs), and other electric utilities [83].Xuelin Yang et al. re- ported the fabrication of porous Cu_2S nanostructure that directly grows on Cu foam via a novel low tem- perature dry thermal sulfuration method [84]. The electrochemical performance of the Cu_2S/Cu as cath- ode for Li-ion battery was studied by charge/discharge test and cyclic voltammetry (CV) measurement. The results indicate that the Cu_2S/Cu cathode exhibits excellent cycle stability and rate capability. When applying a charge/discharge rate of 0.25 C, it delivers initial discharge and charge capacity of 0.74 and

0.40 mAh cm^{-2}, respectively. After 100 cycles, the discharge and charge capacity are both 0.41 mAh cm^{-2}, showing no obvious capacity attenuation. Besides, even after 140 cycles at various rates from 0.3 C to

60 C, the discharge capacity of the Cu_2S/Cu cathode can restore 97.8% when lowering the charge/discharge rate to 0.3 C. The excellent rate capability and cycle stability of Cu_2S/Cu cathode sug- gest that metal sulfides have potential application in high-rate Li-ion batteries, and improving of initial coulombic efficiency may be an important issue to be resolved.

One of the serious problems of the Li/CuS batteries is a rapid drop in capacity during cycling [85, 86] which is caused by the high solubility (in organic solvent electrolytes) of the Li_2S that are formed during the charge/discharge processes [87]. The dissolution of the products in the charge–discharge proc- esses can lead to low active materials utilization, low coulombic efficiency and short cycle life of theCuS cathode [88]. In order to solve these problems, the two approaches were employed for improving the cycle life of CuS cathode. One is the replacement of liquid electrolyte with inorganic solid electrolyte [89]; the other is limiting the discharge cut-off voltage to avoid the formation of Li_2S.

Yourong Wang et al. [87] reported for the first time, the in situ preparation of the CuS cathode on the Cu foil substrate for lithium ion battery by a facile method, and the electrochemical properties of the obtained CuS cathode were investigated under different current density. The possible mechanism of the unique stability of the CuS cathode was discussed. Hierarchical-structured copper sulfide/multi-walled carbon nanotubes (CuS/MWCNTs) are synthesized via a one-step hydrothermal process [90]. As ex- pected, the CuS-MWCNTs exhibit a much higher specific capacitance up to 2831 F g^{-1}, compared with

925.1 F g^{-1} for CuS and 555.6 F g^{-1} for MWCNTs. Furthermore, the CuS-MWCNTs hybrids also exhibit good cycling stability with more than 90% capacitance retention over 600 cycles. The enhancement of CuS/MWCNTs in supercapacitor performance not only attribute to their unique 3D structures with large specific surface area, but also their excellent conductivity, which facilitate efficient charge transport and promotes electrolyte diffusion.

An oriented attachment and growth mechanism allows an accurate control of the size and mor- phology of $Cu_{2-x}S$ nanocrystals, from spheres and disks to tetradecahedrons and dodecahedrons [91]. The performance of $Cu_{2-x}S$ nanocrystals as a cathode in all-vanadium redox flow batteries (VRB) was also tested. The efficiency of this type of battery is usually limited by the rate and potential of the $[VO]^{2+}/[VO_2]^{+}$ cathodic reaction. $Cu_{2-x}S$ nanocrystals were thoroughly purified, deposited on a substrate and fixed by Nafion. Their electrochemical activity was characterized in an inert atmosphere by means of cyclic voltanmetry. Their characteristics were compared with those obtained for a polyacrylonitrile (PAN)-derived graphite felt, which is a material widely used as a VRB cathode. Lower oxidation poten- tials were systematically obtained for $Cu_{2-x}S$ nanocrystals when compared to the PAN-based graphite felt. At a 2 mV s^{-1} scan rate, the oxidation potential was found at 0.72 V for the PAN-based graphite felt and at 0.44 V for the electrode containing $Cu_{2-x}S$ nanocrystals. This result denotes faster electrocatalytic kinetics of the oxidation process for the electrode containing $Cu_{2-x}S$ nanocrystals. The difference of po- tential between the oxidation and reduction peaks was 0.36 V for the PAN-based graphite felt and 0.10 V for the $Cu_{2-x}S$ electrode. Furthermore, the ratio between the currents at the oxidation and reduction peaks for $Cu_{2-x}S$ nanocrystals was close to unity and changed moderately with the scan rate. These experimen- tal results pointed towards a significant performance improvement in terms of reversibility of the $[VO]^{2+}/[VO_2]^{+}$ redox process with the use of $Cu_{2-x}S$ nanocrystals [91]. However, the currents measured with $Cu_{2-x}S$ cathodes were lower than those obtained with PAN-based graphite felts.

2.1.2. Fuel cells. As devices for directly converting chemical energy into electrical energy, fuelcells that oxidize fuel at the anode and reduce oxygen from the air at the cathode to produce electricity for automotive propulsion have achieved great progress in many technical aspects related to their large- scale practical applications [92]. Efficient catalysts for the oxygen reduction reaction (ORR; $O_2 + 4H^+ + 4e^- \rightarrow 2H_2O$) are essential for the fabrication of high performance direct methanol fuel cells (DMFCs) [92]. Many nanomaterials (NMs) such as nitrogen-doped carbon [93,94], CuS [95,96] have been pre- pared and employed as effective catalysts for high-rate ORR kinetics by taking advantage of their large surface area and high catalytic activities [97]. Low-cost MS (M = Co and Cu) exhibits metal-like electri- cal conductivity, a property that has attracted significant interest in electrochemistry; however, current MS electrodes have much lower ORR activities than Pt electrodes [7, 98]. Carbon supports are com- monly used in fuel cells to improve the electrochemical activity and stability of catalysts mainly because of their large surface area, low cost, and unique electrical properties [99]. Carbon-supported Co_3S_4 and $CoSe_2$ NMswith onset potential values of 0.67 V and 0.72 V, respectively, are more active in the ORR than a reversible hydrogen electrode in acidic media [7, 98].

2.1.3. Solar cells. Cu_2S nanoparticles or nanowires could also be grown on carbon or Cu substrates, and the nano devices fabricated using binding of Cu_2S with the conductive substrates may lead to more excellent performance in solar cells and the sensors [50]. In the copper sulfide family, there are several known solid phases like Cu_2S (β, γ -chalcocite), $Cu_{1.96}S$ (djurleite), $Cu_{1.8}S$ (digenite), and CuS (covellite). All of these phases have been identified as p-type semiconducting materials because of the copper vacan-cies within the lattice [49]. Among them, Cu_2S is both an indirect and direct band gap materials, with $Eg_{bulk} \approx 1.2$ eV and 1.8 eV, respectively [100,101], and considered as an ideal absorber in photovoltaic conversions due to its high absorption coefficient (10^4 cm^{-1}) [100] has been widely used in solar cell de- vices.

Cu_2S nanocrystalline films have been successfully prepared using dip-coating technique [102]. Theabsorption coefficient of Cu_2S film in the UV–vis spectrum of the Cu_2S, exhibits a high absorption char- acteristic. The absorption coefficient of spectrum is in the range 10^4 cm^{-1}–10^5 cm^{-1}. This feature is desir- able for the photovoltaic devices applications. Furthermore, it is attractive as a selective solar absorber since it has a high solar absorbency and a low thermal emission [103].

Jeunghee Park et al. fabricated the solar cells and the amperometric glucose sensors using these Cu_2S–MWCNT hybrid nanostructures respond more sensitively than those using the Cu_2S NCs (or MWCNTs) alone. [50,59] The solar cells and the amperometric glucose sensors fabricated using these Cu_2S–MWCNT hybrid nanostructures respond more sensitively than those using the Cu_2S NCs (or MWCNTs) alone. The utilization of the active Cu_2S NCs through direct binding with the conductive MWCNTs would lead to excellent performance of these nanodevices [50]. Su-Huai Wei et al. [104] find that under Cu-rich condition, the anilite $Cu_{1.75}S$ is the most stable structure. It has a predicted band gap of1.4 eV and could a promising solar cell absorber. With a direct energy bandgap of 1.5 eV approachingthe most appropriate range for high photovoltaic conversion and a high absorption coefficient of more than 10^4 cm^{-1}, CuInS has been regarded as a promising candidate for thin film solar cell applications [105]. Solar energy conversion efficiencies above 10% have been obtained with CuInS devices [106]. Using these thin films for the absorption layer of solar cells have attracted growing attention from poly- crystalline ternary semiconductors [107] due to its wide band gap, high absorption coefficient, broad spectrum absorption, and high thermal stability [108].

3. Summary and perspective. In this review, we aim to provide a summary on the properties and perspective applications of nanostructured copper sulfide materials. Controlling copper sulfide nanocrys- tals with an appropriate crystal size is also important. Bigger crystal sizes will lead to smaller specific surface areas and thus lower activity, while smaller sizes often suffer from faster collapse in the crystal- line structure and thus lower stability.

Recent advances have proved that nanostructured copper sulfide materials are great potential mate- rials for energy conversion and storage utilization because of their unique physical and chemical proper- ties and because of the above listed "nanoscale effects". The huge energy requirement and fossil-fuel induced environmental pollution create an enormous strain for scientists to develop clean and sustainable technologies to provide abundant energy in an economically viable way. Energy conversion and storage devices such as fuel cells, photoelectrochemical water splitting cells, solar cells, Li-ion batteries and su percapacitors, etc. have the capability to power the energy demanding areas that range from portableelectronics to transportation and even stationary.

References

1. Lindroos S, Arnold A, Leskela M. Growth of CuS thin films by the successive ionic layer ad- sorption and reaction method // Applied Surface Science. 2000. V. 158, P. 75–80.
2. Lin M.Ch, Lee M.V. $Cu_{2-x}S$ quantum dot-sensitized solar cells // Electrochemistry Communi- cations. 2011, V. 13, P. 1376–1378.
3. Joseph M. Luther, Prashant K. Jain, Trevor Ewers. A. Paul Alivisatos. Localized surface plasmon resonances arising from free carriers in doped quantum dots // Nature Materials. 2011, V. 10, P. 361–366.
4. Qian L, Mao J, Tian X, Yuan H, Xiao D. In situ synthesis of CuS nanotubes on Cu electrode for sensitive nonenzymatic glucose sensor // Sensors and Actuators B. 2013, V. 176, P. 952– 959.
5. Wu Ch, Yu Sh. H., Chen Sh, Liu G, Liu B. Large scale synthesis of uniform CuS nanotubes in ethylene glycol by a sacrificial templating method under mild conditions // J. Mater. Chem. 2006, V. 16, P. 3326–333.
6. Roy P, Srivastava S. K. Hydrothermal growth of CuS wires from Cu-dithiooxamide, a novel single source precursor // Crystal Growth and Design. 2006, V. 6, P. 1921-1926
7. Lai C.H, Huang K.W, Cheng J.H, Lee C.Y, Hwang B.J, Chen L.J. Direct growth of high-rate capability and high capacity copper sulfide nanowire array cathodes for lithium-ion batteries // J. Mater. Chem. 2010, V. 20, P. 6638–6645.
8. Yu X, An X. Controllable hydrothermal synthesis of Cu_2S nanowires on the copper substrate // Materials Letters. 2010, V. 64, P. 252–254.
9. [9]. Roy P, Mondal K, Srivastava S.K. Synthesis of twinned CuS nanorods by simple wet chemical method // Crystal Growth and Design. 2008, V. 8, P. 1530-1534.
10. Roy P, Srivasta S.K. Low-temperature synthesis of CuS nanorods by simple wet chemical method // Mater. Lett. 2007, V. 61, P. 1693–1697.
11. Jiang X, Xie Y, Lu J, He W, Zhu L, Qian Y. Preparation and phase transformation of nanocrystalline copper sulfdes (Cu_9S_8, Cu_7S_4 and CuS) at low temperature // J. Mater. Chem. 2000, V. 10, P. 2193.
12. Zhu T, Xia B.Y, Zhou L,Lou X. W. Arrays of ultrafine CuS nanoneedles supported on a CNT backbone for application in supercapacitors // J. Mater. Chem. 2012, V. 22, P. 7851–7855.
13. Kundu J, Pradhan D. Influence of precursor concentration, surfactant and temperature on the hydrothermal synthesis of CuS: structural, thermal and optical properties // NewJ.Chem. 2013, V. 37, P. 1470-1478.
14. Lim W.P, Wong C.T, Ang S.L, Low H.Y, Chin W.S. Phase-Selective Synthesis of Copper Sulfide Nanocrystals // Chemistry of Materials. 2006, V. 18, P. 6170–6177.
15. Xu H, Wang W, Zhu W. Sonochemical synthesis of crystalline CuS nanoplates via an in situ template route // Materials Letters. 2006, V. 60, P. 2203–2206.
16. Ji R, Wang L, Wang G, Zhang X. Synthesize thickness copper (I) sulfide nanoplates on cop- per rod and its application as nonenzymatic cholesterol sensor // Electrochimica Acta. 2014, V. 130, P. 239–244.

17. Zhang H, Zhang Y, Yu J, Yang D. Phase-selective synthesis and self-assembly of monodis- perse copper sulfide nanocrystals // Journal of Physical Chemistry C. 2008, V. 112, P. 13390–13394.
18. Zhang J, Yu J, Zhang Y, Li Q, Gong J.R. Visible light photocatalytic H_2-production activity of CuS/ZnS porous nanosheets based on photoinduced interfacial charge transfer // Nano Lett. 2011, V. 11, P. 4774–4779.
19. Xua L, Chena X, Mab L, Gao F. Facile preparation of copper sulfide nanoparticles from perovskite templates containing bromide anions // Colloids Surf. A. 2009, V. 349, P. 69–73.
20. Li Z, Fangqi T, Zhao Q, Xianlong Z, Yuhong Y, Juncheng H. Bubble template synthesis of copper sulfide hollow spheres and their applications in lithium ion battery // Materials Letters. 2012, V. 68, P. 28–31.
21. Nagarathinam M, Saravanan K, Leong W.L, Balaya P, Vittal J.J. Hollow nanospheres and flowers of CuS from self-assembled Cu(II) coordination polymer and hydrogen- bonded complexes of N-(2-Hydroxybenzyl)-l-serine. Cryst Growth Des 2009, V. 9, P. 4461–4470.
22. Z.H. Yang, D.P. Zhang, W.X. Zhang, M. Chen, Controlled synthesis of cuprous oxide nano- spheres and copper sulfide hollow nanospheres. J. Phys. Chem. Solids 70 (2009) 840–846.
23. Y. Wang, Y. Hu, Q. Zhang, J. Ge, Z. Lu, Y. Hou, Y. Yin, One-Pot Synthesis and Optical Property of Copper(I) Sulfide Nanodisks. Inorganic Chemistry 49 (2010) 6601–6608.
24. Shaodong S, Zhimao Yang. Cu_2O-templated strategy for synthesis of definable hollow archi- tectures. Chem. Commun., 2014, 50, 7403-7415.
25. Jiao S, Xu L, Jiang K, Xu D. Well-defined non-spherical copper sulfide mesocages with sin- gle-crystalline shells by shape-controlled Cu_2O crystal templating // Adv. Mater. 2006, V. 18, P. 1174– 1177.
26. Ramli E, Rauchfuss T.B, Stern C.L. Interception of copper polysulfide clusters in the reaction of copper and sulfur in donor solvents: polysulfide complexes as the link between molecular and non- molecular metal sulfides // J. Am. Chem. Soc. 1990, V. 112, P. 4043-4044.
27. Motomichi I, Catalina C.V, Michiko B.I. Quintus F. Electroconducting transparent film of amorphous copper sulfide on polyethylene substrate // J. Mater. Chem., 1992, V. 2, P. 761-762.
28. Anuar K, Zainal Z, Hussein M.Z, Saravanan N, Haslina I. Cathodic electrodeposition of Cu_xSthin film for solar energy conversion // Sol. Energy Mater. Sol. Cells. 2002. V. 73, P. 351-365.
29. Dinsmore A.D, Hsu M.F, Nikolaides M.G, Marquez M, Bausch A.R. Weitz DA. Colloi- dosomes: selectively permeable capsules composed of colloidal particles // Science 2002, V. 298, P. 1006–1009.
30. Bigi A, Boanini E, Walsh D, Mann S. Morphosynthesis of octacalcium phosphate hollow mi-crospheres by polyelectrolyte-mediated crystallization // Angew Chem Int Ed 2002, V. 41, P. 2163–2166.[31].
31. Liu B, Zeng H.C. Mesoscale organization of CuO nanoribbons: formation of “Dandelions” //J Am Chem Soc 2004, V. 126, P. 8124–8125.
32. Nakai I, Sugitani T, Nagashima K, Niwa Y. X-ray photoelectron spectroscopic study of cop- per minerals // J. Inorg. Nucl. Chem. 1978, V. 40, P. 789.
33. Folmer J.C.W, Jellinek F. The valence of copper in sulphides and selenides: An X-ray photo- electron spectroscopy study // J. Less Common metals 1980, V.76, P. 153.
34. Westrum E.F, Stolen S, Gronvold F. Thermodynamics of copper sulfides. 2. Heat-capacity and thermodynamic properties of synthetic covellite, CuS, from 5-K to 780.5-K—Enthalpy of decompo- sition // Journal of Chemical Thermodynamics. 1987, V. 19, P. 1199–1208.
35. Potter R.W. An electrochemical investigation of the system copper-sulfur // Econ. Geol. 1977, V. 72, P. 1524.
36. Okamoto K, Kawai S, Kiriyama R. Jap. Electrical and Magnetic Properties of Cu_2Se_2 and Some Related Compounds // J. Appl. Phys. 1969, V. 8, P. 718-724.
37. An C, Wang S, He J, Wang Z. A composite-surfactantsassisted-solvothermal process to cop- per sulfide nanocrystals // J. Cryst. Growth. 2008, V. 310, P. 266–269. http://dx.doi.org/10.1016/j.jcrysgro.2007.11.017
38. Sheng W, Kim S, Lee J, Kim S.W, Jensen K, Bawendi M.G. In-situ encapsulation of quantum dots into polymer microspheres // Langmuir. 2006, V. 22, P. 3782–3790.
39. Orphanou M, Leontidis E, Leodidou T.K, Koutsoukos P, Kyriacou K.C. Study of copper sul- fide crystallization in PEO−SDS solutions // Langmuir. 2004, V. 20, P. 5605-5612.
40. Klimov V, Bolivar P.H, Kurz H, Karavanskii V, Korkishko Y. Linear and nonlinear transmis- sion of Cu_xS quantum dots // Appl. Phys. Lett. 1995, V. 67, P. 653-655.
41. Yin Y, Alivisatos A. P. Colloidal nanocrystal synthesis and the organic–inorganic interface // Nature 2005, V.437, P. 664–670.
42. Wei X , Kong T, Zhu H, Wang L. CuS/Cu_2S nanofluids: Synthesis and thermal conductivity // International Journal of Heat and Mass Transfer. 2010, V. 53, P. 1841–1843.
43. Hsu Y.K, Chen Y.C, Lin Y.G, Chen L.C, Chen K.H. High-cell-voltage supercapacitor of carbon nanotube/carbon cloth operating in neutral aqueous solution // J. Mater. Chem. 2012, V. 22, P. 3383-3387.
44. Hsu Y.K, Chen Y.C, Lin Y.G. Synthesis of copper sulfide nanowire arrays for high- performance supercapacitors // Electrochimica Acta 2014. V. 139, P. 401–407.

45. Yamakawa N, Jiang M, Grey C.P. Investigation of the conversion reactionmechanisms for binary copper(II) compounds by solid-state NMR spectroscopy and X-ray diffraction // Chem Mater. 2009, V. 21, P. 3162–3176.
46. Mane R.S, Lokhande C.D. Chemical deposition method for metal chalcogenide thin films //Mater. Chem. Phys. 2000, V. 65, P. 1-31.
47. Erokhina S, Erokhin V, Nicolini C. Microstructure origin of the conductivity differences inaggregated CuS films of different thickness // Langmuir. 2003, V. 19, P. 766-771.
48. Blachnik R, MüllerA. The formation of Cu_2S from the elements: I. Copper used in form ofpowders // Thermochim. Acta 2000, V. 361, P. 31-52.
49. Mukherjee N, Sinha A, Khan G.G, Chandra D, Bhaumik A, Mondal A. A study on the struc- tural and mechanical properties of nanocrystalline CuS thin films grown by chemical bath deposition technique // Materials Research Bulletin. 2011, V. 46, P. 6–11.
50. Wu Y, Wadia C, Ma W, Sadtler B, Alivisatos A.P. Synthesis and photovoltaic application of copper (I) sulfide nanocrystals // Nano Lett. 2008, V. 8, P. 2551–2555.
51. Lee H, Yoon S.W, Kim E.J, Park J. In situ growth of copper sulfide nanocrystals on multi- walled carbon nanotubes and their application as novel solar cell and amperometric glucose sensor mate- rials // Nano Lett. 2007, V. 7, P. 778–784.
52. Johansson J, Kostamo J, Karppinen M, Niinisto L. Growth of conductive copper sulfide thin films by atomic layer deposition // J. Mater. Chem. 2002, V. 12, P. 1022–1026.
53. Grozdanov I, Najdoski M. Optical and electrical properties of copper sulfide films of variable composition // J. Solid State Chem. 1995, V. 114, P. 469–475.
54. Li L, Zhang Y, Fang X.S, Zhai T.Y, Liao M.Y, Sun X.L,Koide Y, Bando Y, Golberg D.WO_3 nanowires on carbon papers: electronic transport, improved ultraviolet-light photodetectors and ex- cellent field emitters // J. Mater. Chem. 2011, V. 21, P. 6525-6530.
55. Lai C.H, Lu M.Y, Chen L. J. Metal sulfide nanostructures: synthesis, properties and applica- tions in energy conversion and storage // J. Mater. Chem. 2012, V. 22, P. 19–30.
56. Zhao B, Li Sh, Zhang Q, Wang Y, Song Ch, Zhang Z, Yu K. Controlled synthesis of Cu_2S microrings and their photocatalytic and field emission properties // Chemical Engineering Journal. 2013, V. 230, P. 236–243.
57. Li S, Yu K, Wang Y, Zhang Z, Song C, Yin H. Cu_2S@ZnO hetero-nanostructures: facile syn- thesis, morphology-evolution and enhanced photocatalysis and field emission properties // Cryst Eng Comm 2013, V. 15, P.1753–1761.
58. Song Ch, Yin H, Zhang N, Li Sh, Zhao B, Yu K. Two-step synthesis of novel Cu_2S nan- oflowers for field emission application // Materials Letters. 2014, V. 137, P. 56–58.
59. Li L, Fang X, Chew H.G, Zheng F, Liew T.H, Xu X. Crystallinity-controlled germanium nanowire arrays: Potential field emitters // Adv Funct Mater 2008, V. 18, P. 1080–1088.
60. Song Ch, Yu K, Li Sh, Yin H, Zhang N, Zhaoa B, Zhu Z. Controlled synthesis of novel rod- like $Cu_{1.81}S$ nanostructures and field emission properties // Applied Surface Science. 2014, V. 315, P. 235–240.
61. Yu K, Zhang Y.S, Xu F, Li Q, Zhu Z.Q, Wan Q. Significant improvement of field emission by depositing zinc oxide nanostructures on screen-printed carbon nanotube films // Appl. Phys. Lett. 2006, V. 88, P. 153123.
62. Gandubert V. J, Torres E, Niemeyer C. M. Investigation of cytochrome P450- modified cadmium sulfide quantum dots as photocatalysts // J. Mater. Chem. 2008, V. 18, P. 3824-3830.
63. Lu M. Y, Lu M. P, Chung Y. A, Chen M. J, Wang Z. L, Chen L. J. Intercrossed sheet-like ga- doped ZnS nanostructures with superb photocatalytic actvitiy and photoresponse // J. Phys. Chem. C. 2009, V. 113, P. 12878-12882.
64. Li F, Wu J, Qin Q, Li Z, Huang X. Controllable synthesis, optical and photocatalytic proper- ties of CuS nanomaterials with hierarchical structures // Powder Technology. 2010, V. 198, P. 267–274.
65. Zhang Z, Wang C.C, Zakaria R, Ying J.Y. Role of particle size in nanocrystalline TiO_2-based photocatalysts // J. Phys. Chem. B. 1998, V. 102, P. 10871–10878.
66. [65]. Ding T.Y, Wang M.S, Guo S.P, Guo G.C, Huang J.S. CuS nanoflowers prepared by a polyol route and their photocatalytic property // Mater. Lett. 2008, V. 62, P. 4529–4531.
67. Saranya M , Santhosh Ch , Ramachandran R, Kollu P, Saravanan P, Vinoba M, Jeong S.K , Grace A.N. Hydrothermal growth of CuS nanostructures and its photocatalytic properties // Powder Technology. 2014, V. 252, P. 25–32.
68. Thuy U.T.D, Liem N.Q, Parlett C.M.A, Lalev G.M , Wilson K. Synthesis of CuS and CuS/ZnS core/shell nanocrystals for photocatalytic degradation of dyes under visible light // Catalysis Communications. 2014, V. 44, P. 62–67.
69. Dittmer W.U, Simmel F.C. Chains of semiconductor nanoparticles templated on DNA //Appl. Phys. Lett. 2004, V. 85, P. 633-635.
70. [Savariraj A.D, Viswanathan K.K, Prabakar K. CuS nano flakes and nano platelets as counterelectrode for quantum dots sensitized solar cells // Electrochimica Acta. 2014, V. 149, P. 364–369.
71. Raj C.J, Kim B.C, Cho W.J, W.G, Seo Y, Yu K.H. Electrochemical capacitor behavior ofcopper sulfide (CuS) nanoplatelets // Journal of Alloys and Compounds 2014, V. 586, P. 191–196.
72. Orphanou M, Leontidis E, Leodidou T.K, Koutsoukos P, Kyriacou K.C. Study of Copper Sul-fide Crystallization in PEO−SDS Solutions // Langmuir. 2004, V. 20, P. 5605-5612.

73. Sartale S.D, Lokhande C.D. Growth of copper sulphide thin films by successive ionic layer adsorption and reaction (SILAR) method // Mater Chem Phys. 2000, V. 65, P. 63–67.
74. Bordiga S, Paze C, Berlier G, Scarano D, Spoto G, Zecchina A, et al. Interaction of N_2, CO and NO with Cu-exchanged ETS-10: A compared FTIR study with other Cu– zeolites and with dispersedCu_2O // Catal Today 2001, V. 70, P. 91–105.
75. [74]. Xie Y, Li Y, Niu L, Wang L, Qian H, Yao W. A novel surface-enhanced Raman scattering sensor to detect prohibited colorants in food by graphene/silver nanocomposite // Talanta. 2012, V. 100, P. 32–37.
76. Khodadoust S, Ghaedi M, Sahraei R, Daneshfar A. Application of experimental design for removal of sunset yellow by copper sulfide nanoparticles loaded on activated carbon // Journal of Indus- trial and Engineering Chemistry. 2014, V. 20, P. 2663–2670.
77. Ghaedi M, Khodadoust S, Sadeghi H, Khodadoust M. A, Armand R, Fatehi A. Application of ultrasonic radiation for simultaneous removal of auramine O and safranine O by copper sulfide nanopar- ticles: Experimental design // Spectrochimica Acta Part A: Molecular and Biomolecular Spectroscopy. 2015, V. 136, P. 1069–1075.
78. Cai X.J, Gao X, Wang L.S, Wu Q, Lin X.F. A layer-by-layer assembled and car-bon nano- tubes/gold nanoparticles-based bienzyme biosensor for cholesteroldetection // Sens. Actuators. B. 2013, V. 181, P. 575-583.
79. Duan M, Peng Y.L, Zhang L.L, Wang X.Y, Ge J, Jiang J.H, Yu R.Q. DNA-stabilized silver nanoclusters with guanine-enhanced fluorescence as a novel indicator for enzymatic detection of choles- terol // Anal. Methods. 2013, V. 5, P. 2182-2187.
80. Park S, Boo H, Chung T.D. Electrochemical non-enzymatic glucose sensors. // Anal. Chim.
81. Acta. 2006, V. 556, P.46-57.
82. Pickup J.C, Hussain F, Evans N.D, Sachedina N. In vivo glucose monitoring: the clinical real- ity and the promise // Biosensors & Bioelectronics. 2005, V.20, P. 1897–1902.
83. Mayorga-Martinez C.C, Guix M, Madrid R.E, Merkoci A. Bimetallic nanowires as electro- catalysts for nonenzymatic real-time impedancimetric detection of glucose // Chemical Communications. 2012, V. 48, P. 1686–1688.
84. Liu J, Xue D.F. Rapid and scalable route to CuS biosensors: a microwave assisted Cu-complex transformation into CuS nanotubes for ultrasensitive nonenzymatic glucose sensor // Journal of Materials Chemistry. 2011, V. 21, P. 223–228.
85. Su X, Wu Q, Zhan X, Wu J, Wei S, Guo Z. Advanced titania nanostructures and compos- ites for lithium ion battery // Journal of Materials Science. 2012, V. 47, P. 2519-2534.
86. Ni Sh, Lv X, Li T, Yang X. Fabrication of Cu_2S cathode for Li-ion battery via a low tempera- ture dry thermal sulfuration method // Materials Chemistry and Physics 2013, V. 143, P. 349-354.
87. Exner I, Hep J. Copper (II) sulfide as cathode active material in secondary lithium batteries // Journal of Power Sources. 1993, V. 44, P. 701-705.
88. Han Y, Wang Y, Gao W. Synthesis of novel CuS with hierarchical structures and its applica- tion in lithium-ion batteries // Powder Technology. 2011, V. 212, P. 64-68.
89. Wang Y, Zhang, Chen X.P, Liao H, Cheng S. In situ preparation of CuS cathode with unique stability and high rate performance for lithium ion batteries // Electrochimica Acta. 2012, V. 80, P. 264– 268.
90. Ji X, Evers S, Black R, Nazar L.F. Stabilizing lithium-sulphur cathodes using polysulphide reservoirs // Nature Communications. 2011, V. 2, P. 325-331.
91. Yan J.M, Huang H.Z, Zhang J, Liu Z.J, Yang Y. A study of novel anode material CoS_2 for lithium ion battery // Journal of Power Sources. 2005, V. 146, P. 264-269.
92. Huang K.J, Zhang J.Z, Xing K. One-step synthesis of layered CuS/multi-walled carbon nano- tube nanocomposites for supercapacitor electrode material with ultrahigh specific capacitance // Electro- chimica Acta. 2014, V. 149, P. 28–33.
93. Li W, Shavel A, Guzman R, Rubio-Garcia J, Flox C, Fan J, Cadavid D, Ibanez M, Arbiol J, Morante JR, Cabot A. Morphology evolution of $Cu_{2-x}S$ nanoparticles: from spheres to dodecahedrons // Chem. Commun. 2011, V. 47, P. 10332–10334.
94. Gewirth A.A, Thorum M.S. Electroreduction of dioxygen for fuel-cell applications: materials and challenges // Inorganic Chemistry. 2010, V. 49, P. 3557–3566.
95. Shanmugam S, Osaka T. Efficient electrocatalytic oxygen reduction over metal free-nitrogen doped carbon nanocapsules // Chemical Communications. 2011, V. 47, P. 4463–4465.
96. Morozan A, Jousselme B, Palacin S. Low-platinum and platinum-free catalysts for the oxygen reduction reaction at fuel cell cathodes // Energy Environment Science 2011, V. 4, P. 1238– 1254.
97. Wang Y, Li Q, Nie M, Li X, Li Y, Zhong X. High-yield room temperature route to copper sul- fide hollow nanospheres and their electrochemical properties // Nanotechnology. 2011, V. 22, P. 305401-305407.
98. Feng Y, He T, Alonso-Vante N. In situ free-surfactant synthesis and ORR- electrochemistry ofcarbon-supported Co_3S_4 and $CoSe_2$ nanoparticles // Chemistry of Materials. 2008, V. 20, P. 26–28.
99. Steele B.C.H, Heinzel A. Materials for fuel-cell technologies // Nature. 2001, V. 414, P. 345–
100. 352.
101. Wang H, Liang Y, Li Y, Dai H. $Co_{(1-x)}S$-Graphene hybrid: A high-performance metal chalco-genide electrocatalyst for oxygen reduction // Angewandte Chemie International Edition 2011, V. 50, P. 10969–10972.

102. Antolini E. Platinum-based ternary catalysts for low temperature fuel cells: Part I. Preparation methods and structural characteristics // Applied Catalysis B: Environmental 2007, V. 74, P. 324–336.
103. Liu G, Schulmeyer T, Brotz J, Klein A, Jaegermann W. Interface properties and band align- ment of Cu_2S/CdS thin film solar cells // Thin solid films 2003, V. 431-432, P. 477-482.
104. He Y, Kriegseis W, Bläsing J, Polity A, Krämer T, Hasselkamp D, Meyer BK, Hardt M, Krost A. (001)-Textured Cu_2S thin films deposited by RF reactive sputtering // J. Appl. Phys. 2002, V.41, P. 4630-4634.
105. Rafea M.A, Farag A.A.M, Roushdy N. Controlling the crystallite size and influence of the film thickness on the optical and electrical characteristics of nanocrystalline Cu_2S films // Materials Re- search Bulletin. 2012, V. 47, P. 257–266.
106. Wemple S.H, DiDomenico M. Theory of the elasto-optic effect in nonmetallic crystals // J. Phys. Rev. B. 1970, V. 1, P. 193-202.
107. Xu Q, Huang B, Zhao Y, Yan Y, Noufi R, Wei S.H. Crystal and electronic structures of Cu_xSsolar cell absorbers // Appl. Phys. Lett. 2012, V. 100, P. 061906. [105] Alt M, Lewerenz H.J, Scheer R. CuInS2 thin film growth monitoring by in situ electric conductivity measurements // J. Appl. Phys 1997, V. 81, P. 956-961.
108. Dzionk C, Metzner H, Hessler S, Mahnke H.E. Phase formation during the reactive anneal- ing of Cu–In films in H_2S atmosphere // Thin Solid Films. 1997, V. 299, P. 38-44.
109. Cho JW, Park SJ, Kim W, Min BK, Fabrication of nanocrystal ink based superstrate-type $CuInS_2$ thin film solar cells, Nanotechnology 2012,23,265401.
110. Chen H, Yeh Y.M, Liao C.H, Chen J.Z, Wang C. Removal of CuS phases from electrodepos-ited $CuInS_2$ films // Ceramics International 2014, V. 40, P. 67–72.
111. Wang Y. J, Wilkinson D. P, Zhang J. J. Noncarbon support materials for polymer electrolyte membrane fuel cell electrocatalysts // Chem. Rev., 2011, V. 111, P. 7625–7651.
112. Gao M.R, Xu Y.F, Jiang J, Yu Sh.H. Nanostructured metal chalcogenides: synthesis, modifi- cation, and applications in energy conversion and storage devices // Chem. Soc. Rev. 2013, V. 42, P. 2986-3017.